ADVANCED MATERIALS
www.advmat.de

Materials Views
www.MaterialsViews.com

Direct Writing of Polymer Lasers Using Interference Ablation

Tianrui Zhai, Xinping Zhang, Zhaoguang Pang, and Fei Dou*

Optically pumped polymer lasers[1–8] achieved in a simple and efficient way not only introduce new laser designs and laser sources, but also lay excellent physical and technical bases for the realization of electrically pumped organic lasers. As the most promising solution for polymer lasers, the distributed feedback (DFB) geometry has been investigated extensively.[9–12] A variety of fabrication schemes have been demonstrated to construct the DFB cavities, such as UV embossing,[12] nanoimprint lithography,[13–15] photolithography,[16] soft lithography,[17] liquid imprinting,[18] micromolding,[19] electron beam lithography,[20–22] reactive ion etching,[22,23] and reactive electron-beam deposition.[24] However, a simple and low-cost technique that enables highly reproducible mass fabrication is required for the easy realization and more profound investigation of the polymer lasers based on the DFB configuration.

In this work a direct-writing technique is reported that achieves large-area 1D and 2D DFB polymer lasers. The polymer thin film is exposed to a single-shot illumination of the interference pattern of one UV laser pulse at 266 nm. Thus, the DFB structures consisting of periodically distributed polymer nanowires (1D case) or square lattices of polymer nanoislands (2D case) with a period of about 350 nm are easily produced, which support low-threshold lasing in the green region of the visible spectrum. Different 1D and 2D photonic structures can be written with periodic, quasi-periodic, and even aperiodic patterns, generating various designs of the photonic structures and laser devices. Herein, the direct writing and the lasing behaviors of the 1D grating and 2D square lattices of polymeric semiconductors are demonstrated.

A typical light-emitting conjugated polymer, poly[(9,9-dioctylfluorenyl-2,7-diyl)-alt-*co*-(1,4-benzo-{2,1′,3}-thiadiazole)] (ADS133YE, from American Dye Source, Inc.), is employed as the active material, which produces green light under excitation by a blue or UV laser. During fabrication, a solution of 15 mg mL^{-1} ADS133YE in chloroform is spin-coated onto a fused silica glass substrate (15 mm × 15 mm × 1 mm), producing a thin, solid film with a thickness of 100–200 nm, depending on the speed of spin-coating. Then, the thin-film sample is exposed to the interference pattern of a UV laser pulse for about 6 ns, which corresponds to the pulse length of the UV laser. This induces ablation of the polymer at the bright interference fringes, resulting in the structure used for the 1D polymer lasers. For the fabrication of the 2D structures, we simply rotate the sample and perform a second exposure process, with further exposures performed as required. In this work, the square lattice structures are realized by double exposure with the sample rotated once by 90 degrees. **Figure 1**a,b show the molecular structure and the spectroscopic properties of ADS133YE, respectively. The blue curve in Figure 1b shows that the absorption of ADS133YE is centered at about 470 nm. The red and the black curves are the photoluminescence (PL) spectra of ADS133YE before and after the interference ablation process, respectively, which were measured at the same site on the polymer film with a 355 nm excitation laser. Both of the PL spectra are centered around 560 nm. The black curve is only slightly reduced in amplitude as compared with the red curve, which may result from the reduced amount of the polymer at the ablation site, implying that the transient exposure of the polymer film to the 6 ns UV laser pulse did not lead to the degradation of the remaining polymer. This can be confirmed further by comparison with laser devices that have been fabricated using the conventional technique.

Figure 2a illustrates the experimental setup for interference ablation. The UV laser pulse at 266 nm with a pulse length of

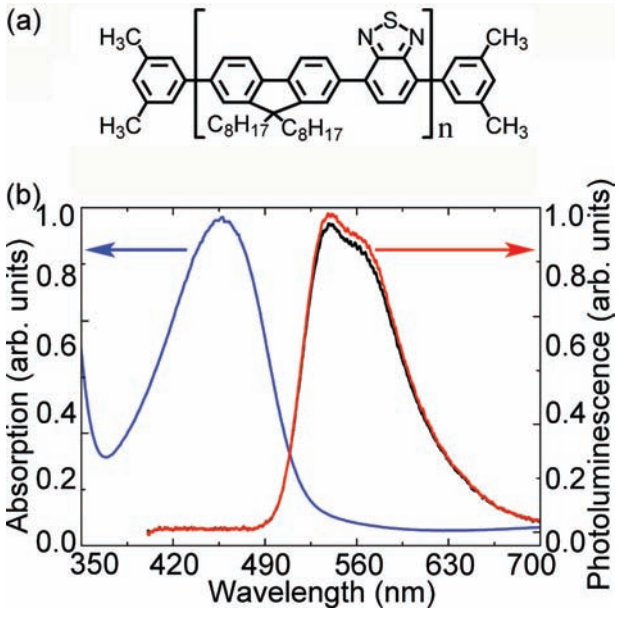

Figure 1. a) The molecular structure of the active polymer semiconductor ADS133YE. b) The absorption (blue curve) and the photoluminescence spectra of ADS133YE before (red curve) and after (black curve) the interference ablation.

Dr. T. R. Zhai, Prof. X. P. Zhang, Dr. Z. G. Pang, F. Dou
Institute of Information Photonics Technology and
College of Applied Sciences
Beijing University of Technology
Beijing 100124, China
E-mail: zhangxinping@bjut.edu.cn

DOI: 10.1002/adma.201100250

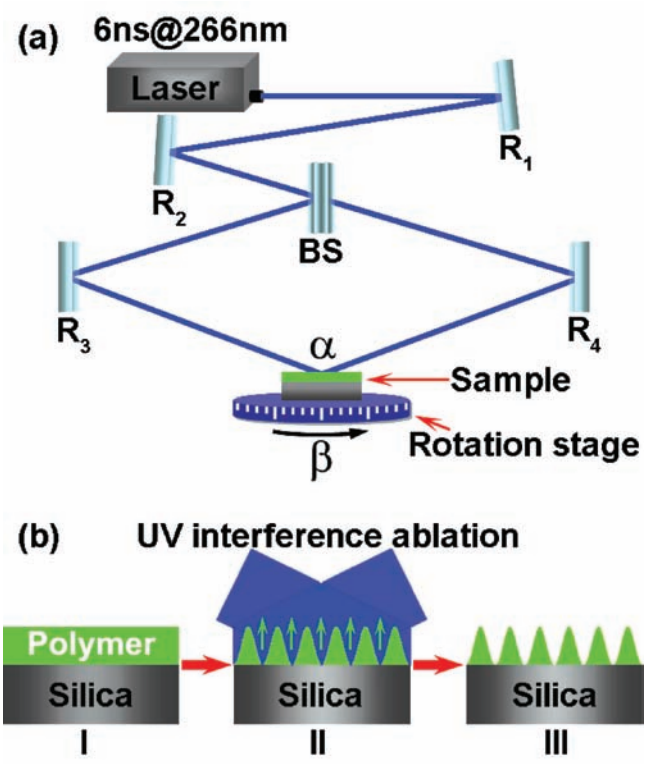

Figure 2. a) The optical layout of the experimental setup for the interference ablation, where R_i (i = 1,2,3,4) denotes the mirrors, BS stands for beam-splitter, α is the angle between the UV laser beams of the two interference arms, β is the orientation angle of the sample controlled by a rotation stage. b) Schematic illustration of the fabrication processes: I. the active polymer (ADS133YE) is spin-coated onto the silica substrate; II. the polymer film is exposed to the interference pattern of a UV laser pulse, where the material at the bright fringes is removed on the timescale equal to the pulse length through an ablation process. Thus, the DFB grating structures of the active organic semiconductor is written directly; III. the resultant grating structures are actually the finished laser device.

about 6 ns and pulse energy of about 20 mJ is split into two beams before being overlapped onto the thin polymeric film sample. After a propagation length of about 2 m, the beam diameter is as large as 5 mm, which approximately describes the effective area of the written structures. The sample to be written is mounted on a rotation stage, which may be rotated about the axis normal to the plane of the substrate. The angle α between the two UV laser beams is changed to control the periods (Λ) of the grating structures by $\Lambda = \frac{\lambda}{2\sin(\alpha/2)}$, where λ is the wavelength of the UV laser and is approximately 45° for the fabrication of the grating with a period of 350 nm. The 2D structures consisting of square lattices are fabricated by a double exposure process with the sample oriented at $\beta = 0$ and 90°. Figure 2b illustrates schematically the interference ablation process. The thin film of the polymeric semiconductor spin-coated onto the glass substrate is illuminated by the interference pattern of the laser pulse at 266 nm. The polymer located at the bright fringes of the interference pattern is "burned" and removed almost immediately within about 6 ns. Since a single pulse is used in the ablation process, the exposure time is exactly equal to the pulse length. Thus, the polymer at the dark fringes remains on the substrate, forming the gratings of the active polymer semiconductors that provide the DFB configuration of the laser device. Experiments show that a pulse energy of about 20 mJ is sufficient to achieve the removal of the polymer at the bright interference fringes.

It should be noted that the ablation taking place during the transient interaction between the intensive UV laser pulse and the polymer film within the area of bright interference fringes produces large amounts of fragments of the polymer material. The size of these pieces is in the range 10–50 nm according to the microscopic measurements, which may fall down to and cover the surface of the grating structures after the ablation process. This may lower the quality of the grating structures and influence the performance of the laser device. Therefore, flowing nitrogen gas over the surface of the sample is necessary to remove this kind of debris and ensures the high-quality of the grating structures.

Figure 3a,b show the atomic force microscopy (AFM) images of the 1D and 2D DFB structures, respectively, directly written using UV interference ablation. Both the 1D and 2D structures have a period of about 350 nm. The modulation depth is about 50 nm for the 1D structures and 100 nm for the 2D structures. The value of the modulation depth is related directly to the thickness of the polymer film, determined by the spin-coating speed. Figure 3 shows excellent images of the photonic structures, which provide strong DFB mechanisms, so that lasing can be achieved at a low pump threshold.

Laser pulses at 355 nm are used as the pump light source, which have a repetition rate of 6.25 kHz and a pulse length of 500 ps and are incident onto the sample at an angle of about 20° after being focused by a lens with a focal length of 100 mm. The spot size of the pump laser on the polymer film is estimated to be about 200 μm in radius. The pump pulse energy is controlled by sending the laser beam through an attenuator wheel. **Figure 4**a,b show the photographs of the lasing actions of the 1D and 2D laser devices, respectively. Strong green laser radiation can be observed when the pump energy is above the threshold. A strip consisting of two arc lines can be observed for the 1D laser and a cross of the arc strips for the 2D device. Most of the laser energy is focused in the center area of the spot. The horizontal profile of the laser beam is defined by the Bragg diffraction of the DFB structures.

The spectroscopic characterization of the output of the 1D laser device is shown in **Figure 5**, where Figure 5a shows the measured spectra of the 1D laser emission at different pump fluences and Figure 5b summarizes the spectral intensity of the laser emission as a function of the pump fluence. The spectra of the laser emission have been measured normal to the substrate. The emission is centered at about 569 nm and has a bandwidth of about 1.3 nm at the full width at half maximum (FWHM). As evaluated from Figure 5b, the pump threshold of this laser is about 130 μJ cm^{-2}, corresponding to a single pulse energy of about 35 nJ.

For comparison, we also measured the output spectra of the 2D laser device at different pump fluences, as shown in **Figure 6**a. The center wavelength of the laser emission is now shifted to about 558 nm. This shorter wavelength (as compared with that of the 1D laser) might be due to the reduced effective refractive index of the Bragg grating, which is evaluated to be

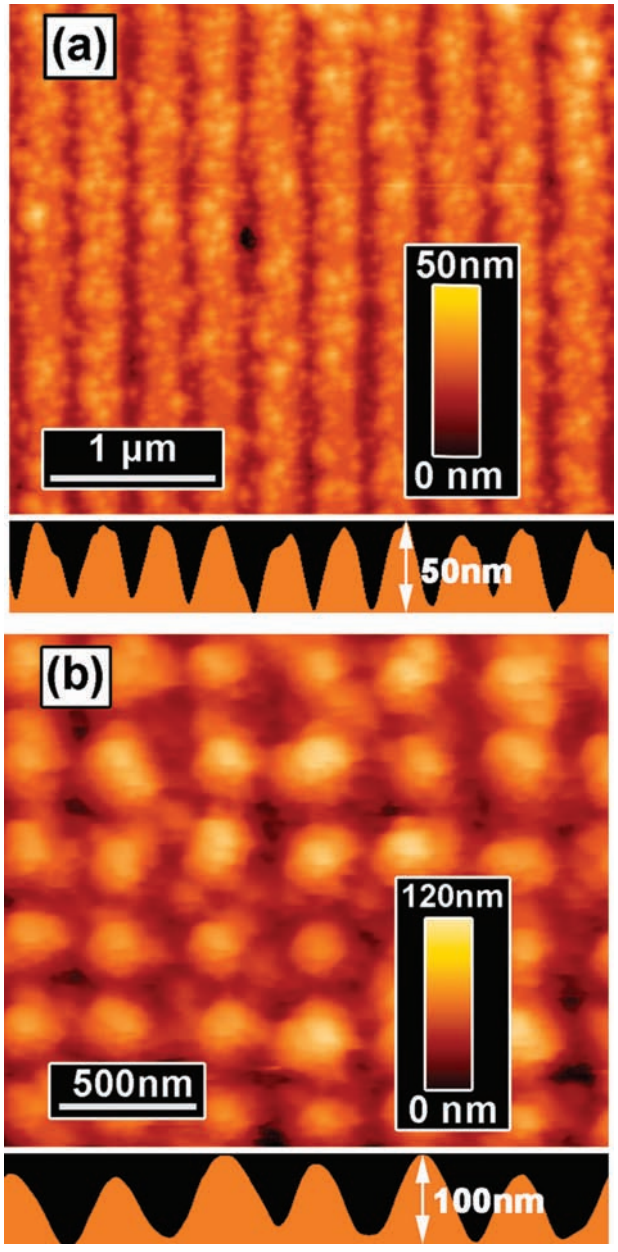

Figure 3. AFM images of the a) 1D and b) 2D DFB structures. The lower panels show the respective averaged profiles.

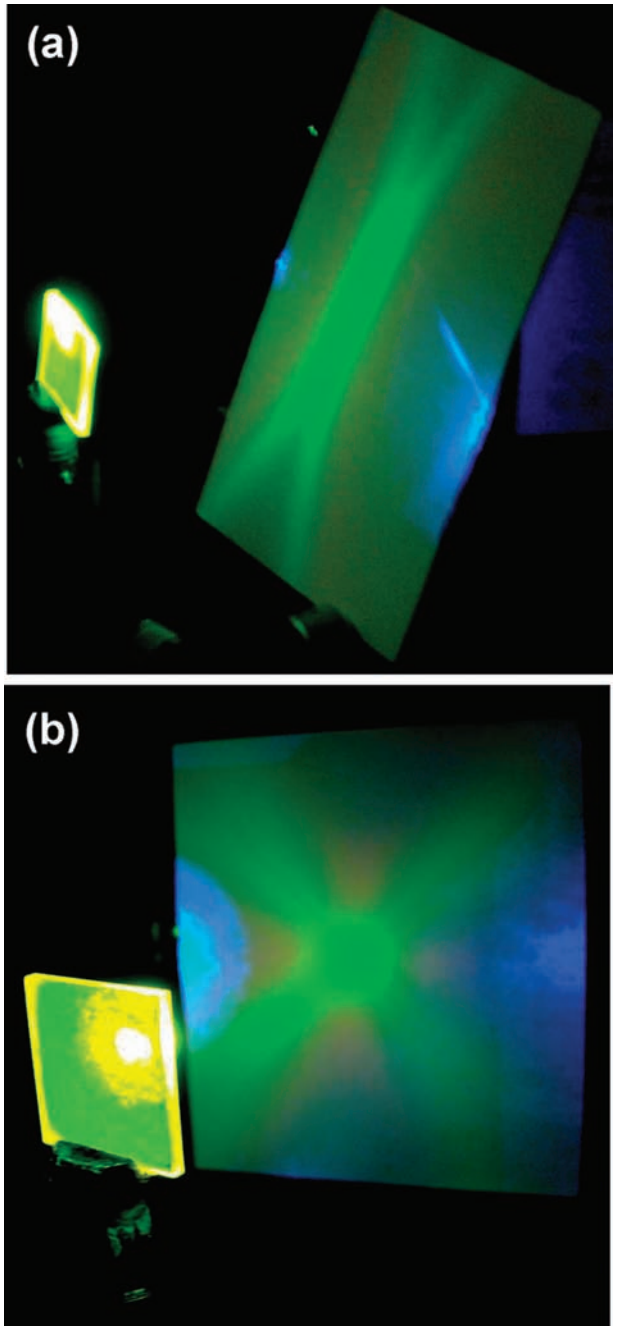

Figure 4. Photographs of the operating polymer laser based on a) 1D and b) 2D DFB gratings.

about 1.59 for the 2D and 1.63 for the 1D Bragg gratings. The laser spectrum has a bandwidth of about 0.9 nm at FWHM. The stronger optical confinement by the 2D feedback might have improved the purity of the laser color. Figure 6b shows how the output laser intensity varies with the pump fluence of the 2D laser, which indicates a pump threshold of about 100 µJ cm^{-2}, corresponding to a single pulse energy of about 27 nJ. Again, the 2D feedback enables more efficient operation of the laser device.

We find in the absorption spectrum shown in Figure 1b that the polymer has an absorbance (at 355 nm) only about 40% of the peak value at about 450 nm. This means that there is still space for improving the quantum efficiency and reducing the pump threshold through optimizing the pump wavelength.

The excellent performance of the directly written polymer lasers implies the success of this new fabrication technique based on single-shot interference ablation. Compared with the conventional fabrication methods—generally requiring nanoimprint lithography or spin-coating the polymeric active medium onto the top of the DFB grating structures—this direct-writing method shows advantages of high simplicity, high reproducibility, and a high success rate.

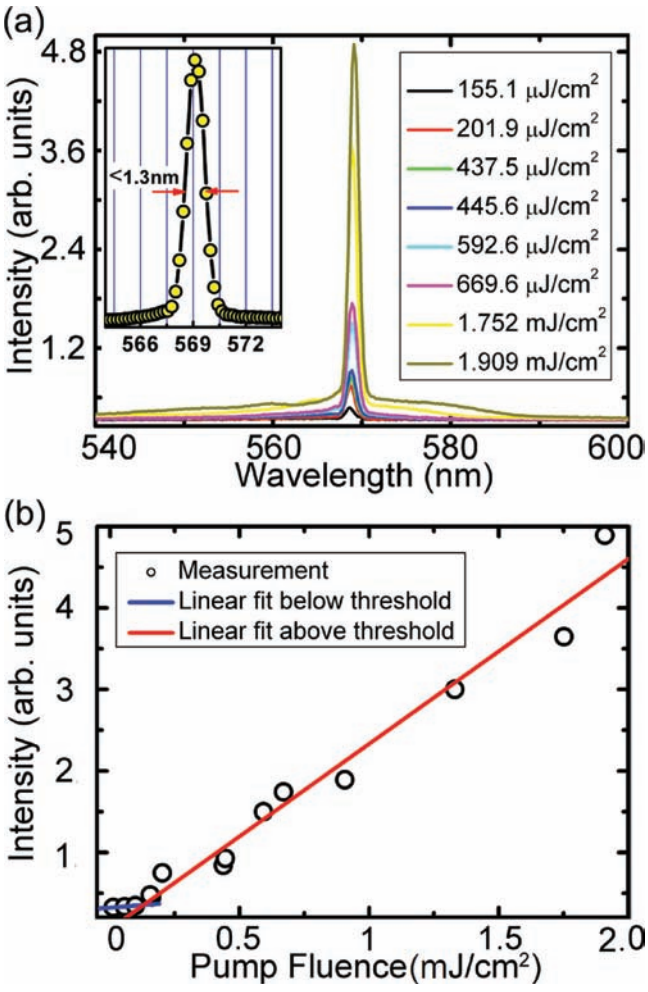

Figure 5. a) Measured spectra of the lasing emission of the 1D polymer laser at different pump fluence, showing a center wavelength of about 569 nm and a linewidth of about 1.3 nm. b) Output intensity of the 1D polymer laser as a function of the pump fluence, indicating a pump threshold of about 130 μJ cm^{-2}.

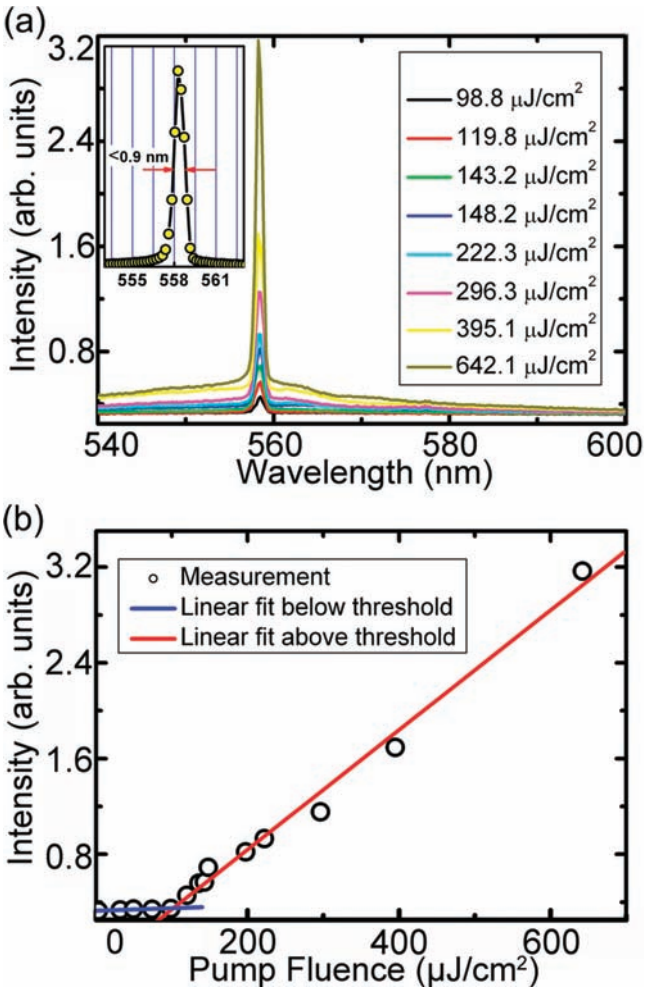

Figure 6. a) Spectra of the emission of the 2D polymer laser at different pump fluences, showing a central wavelength of about 558 nm and a linewidth narrower than 0.9 nm. b) Output intensity of the 2D polymer laser as a function of the pump fluence, indicating a pump threshold lower than 100 μJ cm^{-2}.

Nanoimprint lithography generally involves a series of procedures, which may include fabrication of the master grating, transferring the master grating to a soft stamp, heating the polymer film, and imprinting the DFB structures into the active medium by pressing the stamp onto the solution or the heating-softened film of the polymer semiconductor. The master grating is usually produced by electron-beam lithography, reactive ion etching, or interference lithography, and the achievement of the liquid-processed stamp involves an additional set of procedures. Furthermore, the possible adhesion between the polymer film and the stamp will inevitably lead to a lower-quality copy of the master-grating structures. All of these factors lower the reproducibility and success rate in the realization of the laser device. However, the direct-writing technique based on interference ablation is a single-shot exposure technique involving no complex procedures and no expensive equipment, which can be finished almost instantly, and which demonstrates excellent reproducibility and a high success rate.

Spin-coating of the active polymer on top of a DFB grating is another conventional technique for the simple fabrication of polymer lasers. For a direct comparison with this conventional method, a polymer laser is fabricated by spin-coating the polymer semiconductor ADS133YE onto the photoresist grating that is produced through interference lithography with the performance of this laser (described in the Supporting Information, Figure S1). Clearly, the polymer lasers directly written using interference ablation characterized by Figure 5,6 have lower pump thresholds and narrower emission linewidths than that shown in Figure S1. This implies higher efficiency and better oscillating performance in the directly written lasers, confirming convincingly that the exposure to the short UV laser pulse during interference ablation did not lead to the degradation of the polymeric active medium. Thus, the polymer lasers fabricated using interference ablation have even better performance than those produced by conventional techniques, and are more advantageous due to their easy realization.

In summary, DFB polymer lasers can be simply fabricated by direct writing through UV laser interference ablation. This single-step technique, consisting of single-shot exposure of the polymer film to a single laser pulse, enables mass fabrication of 1D DFB gratings of polymer semiconductors for the realization of laser devices. Furthermore, through multiexposure processes, a variety of 2D patterns can be realized with high reproducibility. Thus, interference ablation introduces a low-cost, high-quality, and large-area fabrication technique for polymer lasers based on DFB mechanisms and for active photonic devices.

Experimental Section

In the experiment, a frequency-quadrupled diode-pumped solid-state laser (Innolas, Spitlight 200) with a pulse length of 6 ns, a center wavelength of 266 nm, and pulse energy of 20 mJ was employed as a laser source for the interference ablation direct writing. The single-shot exposure scheme was used in the interference writing process, with a single output pulse from the laser was used to accomplish the fabrication process. A frequency-tripled diode-pumped solid-state laser (Advanced Optical Technology Ltd.) with a pulse length of 500 ps, a center wavelength of 355 nm, a repetition rate of 6.25 kHz, and a full output power of about 40 mW was employed as the pump laser source. The fabricated DFB structures have a circular effective area with a diameter of about 5 mm on a silica substrate with a total area of 15 mm $\times$ 15 mm and a thickness of 1 mm. The period of the polymer grating structures can be tuned by changing the separation angle (α) between the two UV laser beams and the different patterns of the grating structures can be achieved through multifold exposures by rotating the sample on the rotation stage or changing the angle β. In this work, one- and two-dimensional (square lattices) DFB structures with a period of about 350 nm have been written to achieve the laser devices. The light-emitting polymer ADS133YE was used as the active medium, purchased from American Dye Source, Inc. A SPA-400 AFM was used to characterize the microscopic properties of the fabricated nanostructures and the Ocean Optics Maya 2000 PRO spectrometer is used to measure the spectra of the laser radiation.

Supporting Information

Supporting Information is available from the Wiley Online Library or from the author.

Acknowledgements

The authors acknowledge the High-tech Research and Development Program of China (2007AA03Z306), the National Natural Science Foundation of China (11074018), the Beijing Educational Commission (KZ200810005004), the Program for New Century Excellent Talents in University (NCET), and the Research Fund for the Doctoral Program of Higher Education of China (20091103110012) for the financial support.

Received: January 20, 2011
Published online: March 4, 2011

[1] I. Samuel, G. Turnbull, *Chem. Rev.* **2007**, *107*, 1272.
[2] N. Tessler, G. Denton, R. Friend, *Nature* **1996**, *382*, 695.
[3] W. Holzer, A. Penzkofer, S. Gong, A. Bleyer, D. Bradley, *Adv. Mater.* **1996**, *8*, 974.
[4] C. Kallinger, M. Hilmer, A. Haugeneder, M. Perner, W. Spirkl, U. Lemmer, J. Feldmann, U. Scherf, K. Müllen, A. Gombert, *Adv. Mater.* **1998**, *10*, 920.
[5] M. McGehee, M. Diaz-Garcia, F. Hide, R. Gupta, E. Miller, D. Moses, A. Heeger, *Appl. Phys. Lett.* **1998**, *72*, 1536.
[6] U. Scherf, S. Riechel, U. Lemmer, R. Mahrt, *Curr. Opin. Solid State Mater. Sci.* **2001**, *5*, 143.
[7] C. Bauer, H. Giessen, B. Schnabel, E. Kley, C. Schmitt, U. Scherf, R. Mahrt, *Adv. Mater.* **2001**, *13*, 1161.
[8] M. Song, B. Wenger, R. Friend, *J. Appl. Phys.* **2008**, *104*, 033107.
[9] H. Kogelnik, C. Shank, *J. Appl. Phys.* **1972**, *43*, 2327.
[10] G. Heliotis, R. Xia, G. Turnbull, P. Andrew, W. Barnes, I. Samuel, D. Bradley, *Adv. Funct. Mater.* **2004**, *14*, 91.
[11] G. Kranzelbinder, G. Leising, *Rep. Prog. Phys.* **2000**, *63*, 729.
[12] M. Berggren, A. Dodabalapur, R. Slusher, A. Timko, O. Nalamasu, *Appl. Phys. Lett.* **1998**, *72*, 410.
[13] E. Namdas, M. Tong, P. Ledochowitsch, S. Mednick, J. Yuen, D. Moses, A. Heeger, *Adv. Mater.* **2009**, *21*, 799.
[14] C. Ge, M. Lu, X. Jian, Y. Tan, B. Cunningham, *Opt. Express* **2010**, *18*, 12980.
[15] D. Pisignano, L. Persano, P. Visconti, R. Cingolani, G. Gigli, G. Barbarella, L. Favaretto, *Appl. Phys. Lett.* **2003**, *83*, 2545.
[16] J. Chang, M. Gwinner, M. Caironi, T. Sakanoue, H. Sirringhaus, *Adv. Funct. Mater.* **2010**, *20*, 2825.
[17] B. Scott, G. Wirnsberger, M. McGehee, B. Chmelka, G. Stucky, *Adv. Mater.* **2001**, *13*, 1231.
[18] M. Gaal, C. Gadermaier, H. Plank, E. Moderegger, A. Pogantsch, G. Leising, E. List, *Adv. Mater.* **2003**, *15*, 1165.
[19] J. Lawrence, G. Turnbull, I. Samuel, *Appl. Phys. Lett.* **2003**, *82*, 4023.
[20] D. Pisignano, L. Persano, R. Cingolani, G. Gigli, F. Babudri, G. Farinola, F. Naso, *Appl. Phys. Lett.* **2004**, *84*, 1365.
[21] M. Salerno, G. Gigli, M. Zavelani-Rossi, S. Perissinotto, G. Lanzani, *Appl. Phys. Lett.* **2007**, *90*, 111110.
[22] P. Del Carro, A. Camposeo, R. Stabile, E. Mele, L. Persano, R. Cingolani, D. Pisignano, *Appl. Phys. Lett.* **2006**, *89*, 201105.
[23] G. Turnbull, P. Andrew, M. Jory, W. Barnes, I. Samuel, *Phys. Rev. B* **2001**, *64*, 125122.
[24] L. Persano, A. Camposeo, P. Del Carro, E. Mele, R. Cingolani, D. Pisignano, *Opt. Express* **2006**, *14*, 1951.